

# A Computationally Efficient Electromagnetic Wave Scattering Analysis Method for Electrically Large Multilayered Dielectric Structures

Keerthi K. S.<sup>1</sup>, Parul Mathur<sup>2</sup>, Ilango K.<sup>3</sup> and Dhanesh G. Kurup<sup>2</sup>

<sup>1</sup>Department of Electrical and Electronics Engineering, Amrita Vishwa Vidyapeetham, Amritapuri, India.

<sup>2</sup>RF and Wireless System Laboratory, Department of Electronics and Communication Engineering, Amrita School of Engineering, Amrita Vishwa Vidyapeetham, Bengaluru, India.

<sup>3</sup>Department of Electrical and Electronics Engineering, Amrita School of Engineering, Amrita Vishwa Vidyapeetham, Coimbatore, India.

Corresponding author: Keerthi K. S. (email: keerthiks@am.amrita.edu)

**ABSTRACT** The paper presents a computationally efficient method based on the modified equivalent current approximation for electromagnetic wave scattering analysis of electrically large multilayered lossy dielectric structures. The proposed method can be an effective alternative to commercially available tools and methods, which tend to become computationally intensive with increase in size and losses of structures. The proposed method is applied to compute the radar cross-section(RCS) of various multilayered dielectric and coated perfect electric conductor (PEC) structures for both TE and TM polarization under normal and oblique incidences and compared with the method of moments (MoM) and finite element method (FEM). The result shows excellent agreement and reduced computational resources and time compared to both MoM and FEM. In comparison, the proposed method saves computational time by a factor of 15, and over 50% reduction in memory usage. The proposed method can be applied directly to study scattering problems involving electrically large multilayer dielectric and conducting structures.

**INDEX TERMS** Multilayered scattering, Radar cross-section, Electromagnetic wave scattering, Lossy dielectric medium, Modified equivalent current approximation

## I. INTRODUCTION

A NUMBER of real-world applications, such as material quality testing [1], bio-electromagnetic interactions [2]–[4], stealth and counter-stealth technologies [5], involve electromagnetic wave interactions with electrically large multilayered dielectric structures. Full-wave analysis methods, namely the method of moments (MoM), finite element method (FEM), are widely used for accurate electromagnetic wave scattering analysis [6]–[9]. However, these full-wave analysis methods become computationally complex and unstable with increase in size, number of coatings, number of layers, and losses in dielectric materials [10], [11]. On the other hand, high-frequency methods such as physical optics, geometrical optics, or a combination of the two provide a faster analysis of electrically large surfaces with an admissible reduction in accuracy [12]–[15]. Thus, making the high-frequency method more favorable for efficient scattering analysis for large multilayered structures. Comparing various high-frequency methods, the physical optics (PO) method is the most extensively studied for scattering analysis of electrically large structures. The scattering analysis using PO methods was usually limited by the constraint that the scattering object must be a PEC surface [16]. A surface

discretization-based PO method, modified equivalent current approximation (MECA) method, proposed in [17] addresses this limitation by introducing a non-zero magnetic current in the formulation to account for a lossy homogeneous dielectric scatterer. Further, the method above assumes a constant amplitude current distribution with linear phase fluctuation in the facet. As a result, the size of the facets can be relatively large, which makes the method computationally efficient.

In this paper, we propose an enhancement of the MECA method [17] for multilayer dielectric structures. We introduce an equivalent reflection coefficient method to model the scattering properties of a general multilayer media, which replaces the reflection coefficient of a homogeneous layer in the MECA method, simplifying the complex multilayer structure into an equivalent single-layer structure. Consequently, the computational time for the multilayer structure also gets reduced to that of a single layer, as elaborated in the following sections. Fig. 1 shows a generic multilayer structure for both TE and TM polarization. The equivalent single-layer structure for TE and TM polarization proposed in this paper is shown in Fig. 2. Additionally, the proposed method uses two-dimensional surface meshing compared to three-dimensional meshing in full-wave analysis, making the

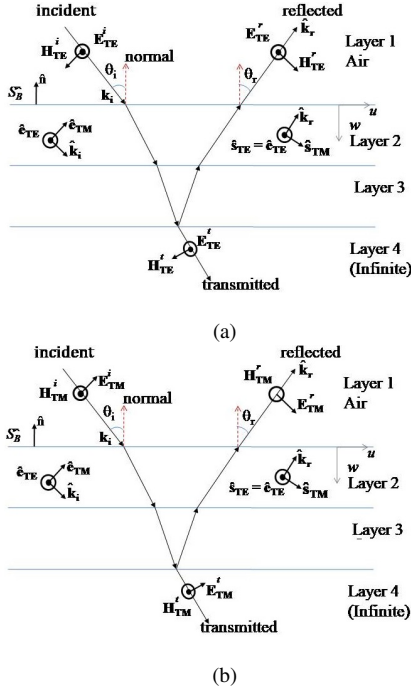


FIGURE 1: Oblique plane wave incidence in multilayer structure (a) TE polarization (b) TM polarization.

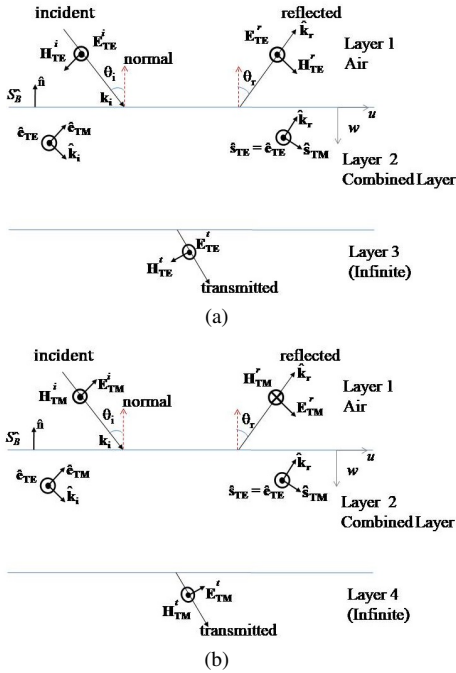


FIGURE 2: Oblique plane wave incidence in the proposed equivalent single-layer structure (a) TE polarization (b) TM polarization.

proposed method more memory efficient.

The organization of the paper is as follows: section II discusses the mathematical formulation of the proposed

method; section III deals with the validation of the proposed method by comparing the computed values of radar cross section (RCS) for different multilayered structures with MoM method, followed by conclusion in section IV.

## II. EQUIVALENT REFLECTION COEFFICIENT BASED MULTILAYER SCATTERING ANALYSIS METHOD

Electromagnetic wave interaction in multilayer structures involves scattering and transmission of electromagnetic waves at multiple interfaces. Computing the total scattered field for the multilayer structure by analyzing the wave interaction at individual interfaces will be computationally intensive. The proposed method overcomes this limitation by modeling the multilayer structure as a single unit using an equivalent reflection coefficient instead of the general dispersion coefficients of individual interfaces. The formulation for finding the equivalent reflection coefficient is based on characteristic matrix method (CMM), which combines the effects of all the interfaces in a multilayered medium to generate an equivalent reflection coefficient [19]. The pivotal step in CMM is determining a matrix  $M_t$ , which depends on the propagation constant for TE and TM polarized electromagnetic waves at individual layers constituting the overall multilayer structure. The matrix  $M_t$  is derived through multiplication of layer-matrices  $M_i$ ,  $i = [2 : N-1]$ , which encapsulates the material properties of individual layers with the first layer ( $i = 1$ ) modeled as vacuum of infinite thickness and the last layer ( $i = N$ ) modeled either as PEC or dielectric media of infinite thickness,

$$M_i = \begin{bmatrix} \cos \delta_i & \frac{j}{\zeta_i} \sin \delta_i \\ j \zeta_i \sin \delta_i & \cos \delta_i \end{bmatrix} \quad (1)$$

where,  $\delta_i$  is given by the following equation.

$$\delta_i = j \gamma_i d_i \cos \theta \quad (2)$$

In (2),  $\gamma_i$  represents the propagation constant of the electromagnetic wave in medium  $i$ ,  $\theta$  is the angle of incidence, and  $d_i$  is the thickness of the  $i^{\text{th}}$  layer. The variable  $\zeta_i$  in (1), called tilted-admittance [20], is a function of polarization, material admittance ( $Y_i$ ) and incident angle  $\theta$  as,

$$\begin{aligned} \zeta_i &= Y_i \cos \theta, \quad (\text{TE polarization}) \\ \zeta_i &= \frac{Y_i}{\cos \theta}, \quad (\text{TM polarization}) \end{aligned} \quad (3)$$

The decomposed reflection coefficients ( $\rho_{TE/TM}$ ) are calculated using corresponding tilted admittance obtained in (3) and elements of  $M_t$  as,

$$\rho_{TE/TM} = \frac{\zeta_1(M_{t11} + M_{t12}\zeta_N) - (M_{t21} + M_{t22}\zeta_N)}{\zeta_1(M_{t11} + M_{t12}\zeta_N) + (M_{t21} + M_{t22}\zeta_N)} \quad (4)$$

where,  $\zeta_1$  and  $\zeta_N$  are tilted admittance of the first and last layer respectively. The decomposed equivalent reflection coefficient obtained in (4) is used along with incident electric and magnetic fields to compute reflected electric field ( $E_{TE}^r$ )

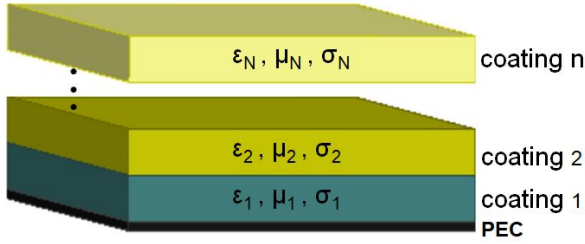


FIGURE 3: PEC plate with multilayer dielectric coating

and  $\mathbf{E}_{\text{TM}}^r$ ) and magnetic field ( $\mathbf{H}_{\text{TE}}^r$  and  $\mathbf{H}_{\text{TM}}^r$ ) of each facet of the mesh, as given in (5).

$$\begin{aligned} \mathbf{E}_{\text{TE}}^r &= E_{TE}^i \rho_{TE} \hat{\mathbf{e}}_{\text{TE}} \\ \mathbf{H}_{\text{TE}}^r &= \frac{1}{\eta_1} E_{TE}^i \rho_{TE} (\hat{\mathbf{k}}_r \times \hat{\mathbf{e}}_{\text{TE}}) \\ \mathbf{E}_{\text{TM}}^r &= E_{TM}^i \rho_{TM} \hat{\mathbf{r}}_{\text{TE}} = E_{TM}^i \rho_{TM} (\hat{\mathbf{k}}_r \times \hat{\mathbf{e}}_{\text{TE}}) \\ \mathbf{H}_{\text{TM}}^r &= \frac{1}{\eta_1} E_{TM}^i \rho_{TM} \hat{\mathbf{e}}_{\text{TE}} \end{aligned} \quad (5)$$

where,  $E_{TE}^i$  and  $E_{TM}^i$  is the magnitude of decomposed incident electric field,  $\eta_1$  is the impedance of first medium and  $\hat{\mathbf{k}}_r = \hat{\mathbf{k}}_i - 2\hat{\mathbf{n}}(\hat{\mathbf{k}}_i \cdot \hat{\mathbf{n}})$  is the unit vector along the direction of reflection for the outward unit normal  $\hat{\mathbf{n}}$ . The direction of the field components is established with local coordinate system defined by the unit vectors  $[\hat{\mathbf{k}}_i, \hat{\mathbf{e}}_{\text{TE}}, \hat{\mathbf{e}}_{\text{TM}}]$  for incident wave and  $[\hat{\mathbf{r}}_{\text{TE}}, \hat{\mathbf{k}}_r, \hat{\mathbf{r}}_{\text{TM}}]$  for reflected wave. The usage of the equivalent reflection coefficient ( $\rho_{TE}/\rho_{TM}$ ) enhances the method to be applicable for multilayer medium.

As mentioned in [17], the electric and magnetic currents are computed for each facet in terms of magnetic and electric fields of the corresponding incident and reflected waves, obtained in (5), and the outward unit normal  $\hat{\mathbf{n}}$  of the facet. This electric and magnetic current is then used to derive the analytical solution of the radiation integral at a far-field observation point for every facet. The summation of which gives the total scattered field.

### III. RESULTS

For the validation of the proposed method, monostatic and bistatic radar cross-section (RCS) of electrically large multilayered dielectric structures is computed, and the results are compared with the method of moments (MoM) [18]. The validation study examines the RCS of multilayered structures with material properties ranging from PEC to lossy dielectric for normal and oblique incidences of plane wave.

Fig. 3, shows the general geometry of the conductor-backed multilayered structure considered for RCS computations in the paper. The structure consists of a PEC layer with  $N$  dielectric coatings of permittivity ( $\epsilon_i$ ), permeability ( $\mu_i$ ) and conductivity ( $\sigma_i$ ) stacked one over the other, where  $i = [1 : N]$ . Structure with curved surface is also included in the study to validate the geometrical inclusiveness of the proposed method. The key metrics of the study are computational efficiency and accuracy of the proposed method.

First, the RCS of a single-coated square plate of side  $5\lambda$  is computed for TE and TM polarized plane wave and validated using MoM. The structure has three layers with an infinite air layer at the top, a dielectric layer ( $\epsilon_r = 1.8$ ,  $\mu_r = 1.5$ ,  $\sigma = 10.2\omega\epsilon_0$  and  $\tan\delta = 5.6$  [17]) of thickness  $0.1\lambda$ , and a thin layer of PEC as the third layer. A comparison of the bistatic RCS for a plane wave of normal incidence and oblique ( $\theta = 30^\circ$ ) incidence is shown in Fig. 4 and Fig. 5 respectively. For normal incidence, the reflected wave is along the angle of incidence as in Fig. 4, with the main lobe or the maximum value of RCS along  $0^\circ$ . The results show that the proposed method is in good agreement with MoM, particularly at observation angles near the angle of incidence. The deviation in RCS for observation angles farther away from the incident angle can be attributed to the fact that the

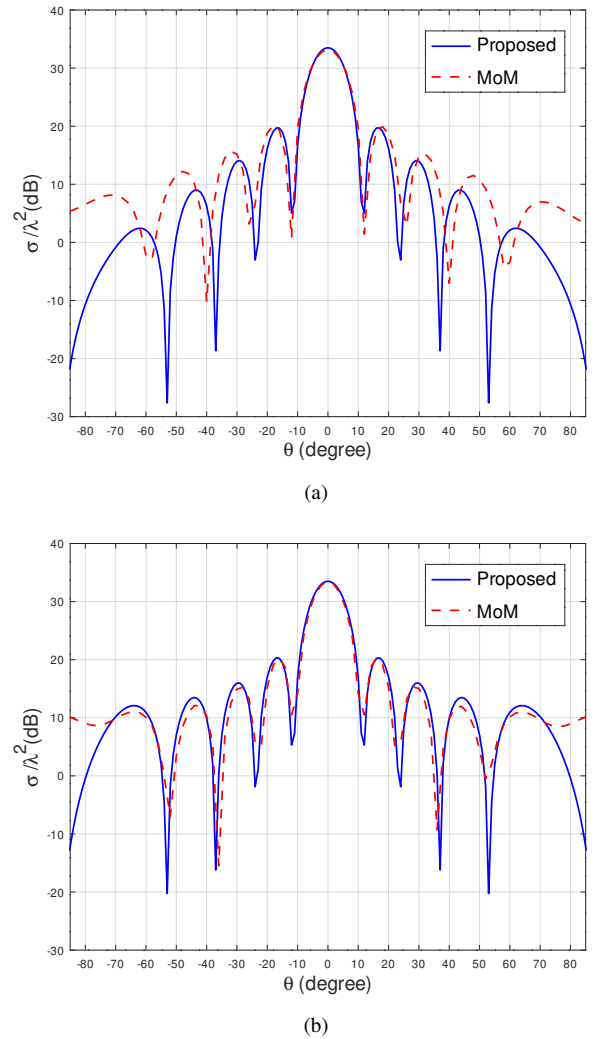
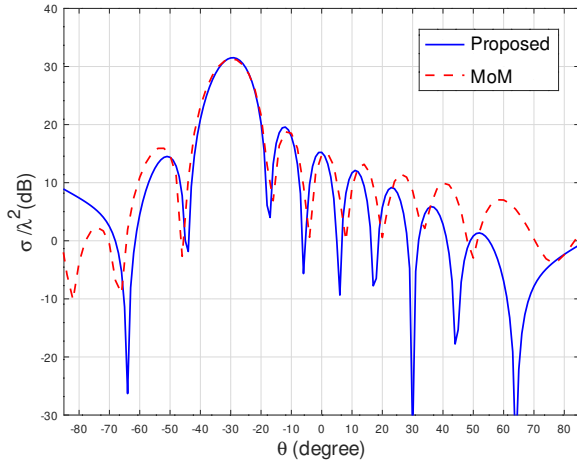
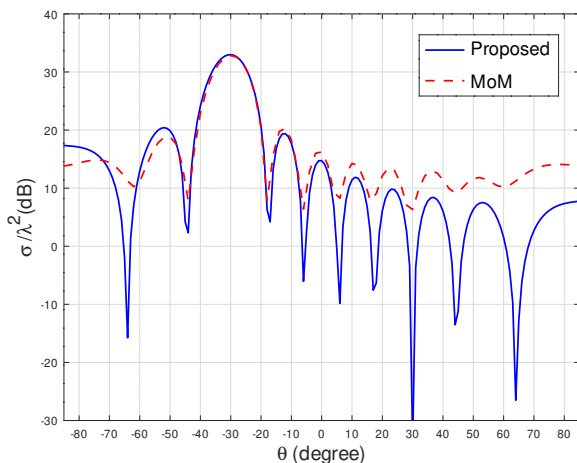


FIGURE 4: Normalized bistatic RCS of coated PEC square plate of side  $5\lambda$  with dielectric coating ( $\epsilon_r = 1.8$ ,  $\mu_r = 1.5$ ,  $\sigma = 10.2\omega\epsilon_0$  and  $\tan\delta = 5.6$ ) w.r.t observation angle  $\theta$  for normal plane wave incidence of a) TE polarization b) TM polarization.



(a)



(b)

FIGURE 5: Normalized bistatic RCS of a coated PEC square plate of side  $5\lambda$  with dielectric coating ( $\epsilon_r = 1.8$ ,  $\mu_r = 1.5$ ,  $\sigma = 10.2\omega\epsilon_0$  and  $\tan\delta = 5.6$ ) w.r.t observation angle  $\theta$  for oblique plane wave incidence of a) TE polarization b) TM polarization.

CMM method used for computing the reflection coefficient is limited to the angle range of  $\pm 80^\circ$ . Furthermore, the deviations can be neglected as the RCS values are much smaller compared to the dominant lobe. For oblique incidence, the maximum value is obtained at the same angle but in the other quadrant, i.e. at an angle  $\approx -30^\circ$  ( $\theta = 30^\circ$ ,  $\phi = 270^\circ$ ), for incident angle  $30^\circ$  ( $\theta = 30^\circ$ ,  $\phi = 90^\circ$ ), which is in consensus with the Snell's law of reflection at the plane interface [21], see Fig. 5.

Next, we study the monostatic RCS for the same single-coated square plate structure to examine the effect of varying coating thicknesses at a constant frequency of 2.45GHz, see Fig. 6. As the coating thickness becomes electrically significant,  $\geq 0.2\lambda$ , the proposed method and MoM yield a constant or nearly constant RCS value respectively. The

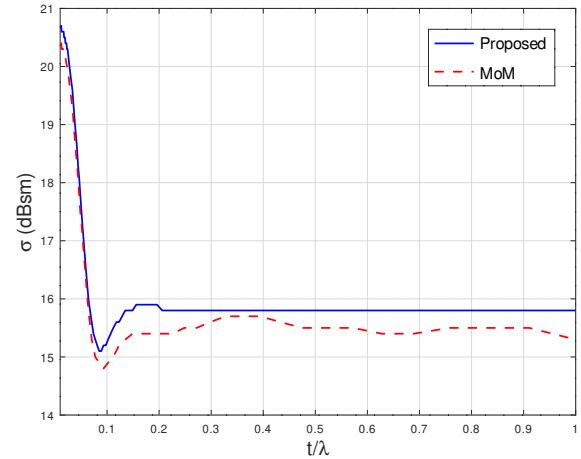


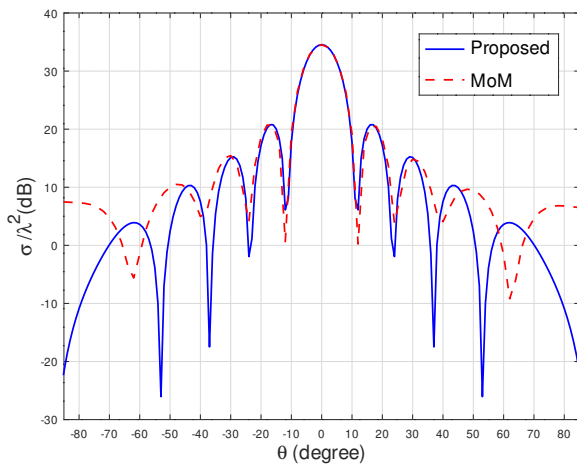
FIGURE 6: Normalized monostatic RCS w.r.t normalized coating thickness for a coated PEC square plate of side  $5\lambda$ ; with dielectric coating of  $\epsilon_r = 1.8$ ,  $\mu_r = 1.5$ ,  $\sigma = 10.2\omega\epsilon_0$  and  $\tan\delta = 5.6$ .

marginal deviation in the RCS is due to the fact that the proposed method is an approximation method, while MoM a full wave analysis method.

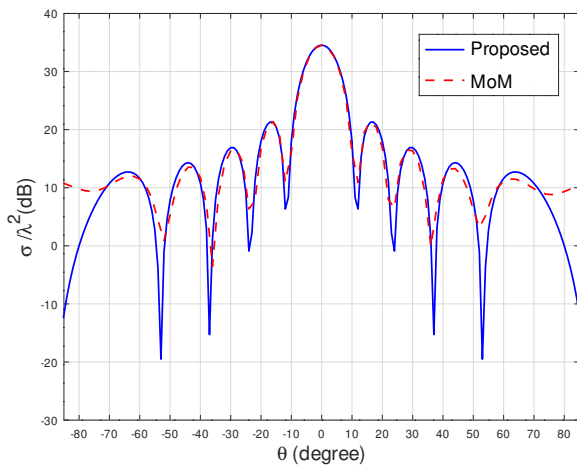
For studying the effect of multilayer coating on RCS, we consider a double-coated square plate of side  $5\lambda$ . The material constants of the first layer of the coating are,  $\epsilon_{r1} = 1.8$ ,  $\mu_{r1} = 1.5$ ,  $\sigma_1 = 10.2\omega\epsilon_0$ ,  $\tan\delta = 5.6$  and thickness  $0.1\lambda$  followed by a second layer with material constants,  $\epsilon_{r2} = 2$ ,  $\sigma_2 = 0.033$  S/m and thickness  $0.2\lambda$ . The bistatic RCS for the double-coated square plate is computed for normal plane wave incidence for TE and TM polarization, see Fig. 7. The result shows that the proposed method is in good agreement with MoM, especially for observation angles closer to the angle of incidence. As stated before, the deviations at the farther ends can be neglected since the RCS values are low compared to the dominant lobe.

For validating the proposed method for curved geometry we consider a dielectric-coated PEC sphere with material properties of the coating,  $\epsilon_r = 1.8$ ,  $\mu_r = 1.5$ ,  $\sigma = 10.2\omega\epsilon_0$  and  $\tan\delta = 5.6$ , see Fig. 8. The monostatic RCS of the coated sphere is computed for normal incidence and varying frequency while keeping the radius of the sphere and coating thickness constant. The results obtained are compared with MoM, see Fig. 9. As can be seen in Fig. 9, the RCS values computed using the proposed method are in good agreement with MoM, especially at higher frequencies. The deviations can be observed at the lower frequencies as the structure becomes electrically small. This is because the proposed method is formulated especially for electrically large structures.

Next, the monostatic RCS for normal plane wave incidence of a solid PEC sphere and a solid sphere with material constants  $\epsilon_r = 1.8$ ,  $\mu_r = 1.5$ ,  $\sigma = 10.2\omega\epsilon_0$  and  $\tan\delta = 5.6$



(a)



(b)

FIGURE 7: Normalized bistatic RCS of a multilayer coated PEC square plate of side  $5\lambda$ , with first dielectric coating of  $\epsilon_{r1} = 1.8$ ,  $\mu_{r1} = 1.5$  and  $\sigma_1 = 10.2\omega\epsilon_0$  and second dielectric coating  $\epsilon_{r2} = 2$  and  $\sigma_2 = 0.033$  S/m w.r.t observation angle  $\theta$  for normal plan wave incidence of a) TE polarization b) TM polarization.

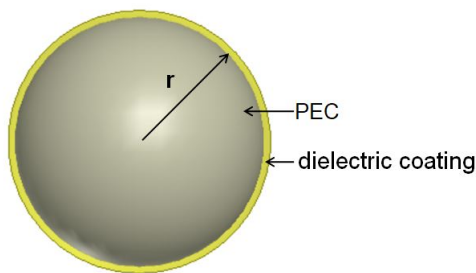


FIGURE 8: Dielectric coated PEC sphere

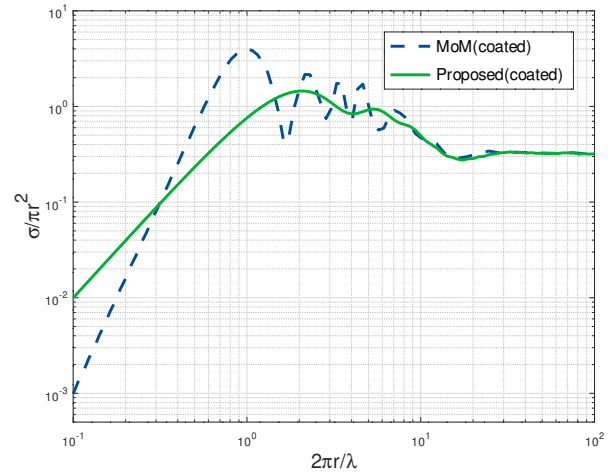


FIGURE 9: Normalized monostatic RCS of a coated PEC sphere with dielectric coating ( $\epsilon_r = 1.8$ ,  $\mu_r = 1.5$ ,  $\sigma = 10.2\omega\epsilon_0$  and  $\tan\delta = 5.6$ ) w.r.t normalized outer circumference for normal plane wave incidence.

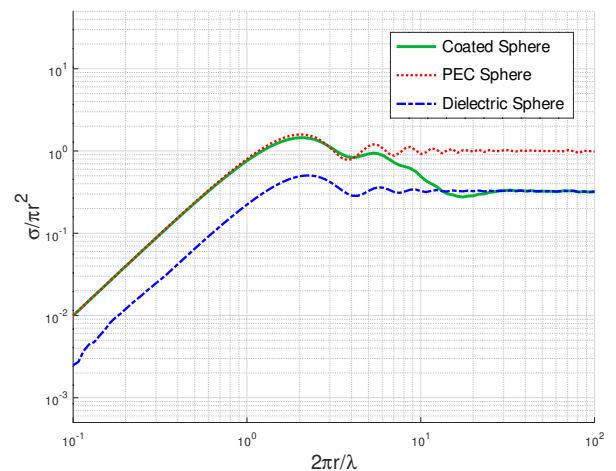


FIGURE 10: Normalized monostatic RCS of solid PEC, solid dielectric( $\epsilon_r = 1.8$ ,  $\mu_r = 1.5$ ,  $\sigma = 10.2\omega\epsilon_0$  and  $\tan\delta = 5.6$ ) and solid PEC sphere with a same dielectric coating w.r.t normalized outer circumference .

is compared with PEC backed coated sphere with thickness  $0.06\lambda$  and same material constants as that of solid sphere, see Fig. 10. As seen the Fig. 10, the coated sphere exhibits an RCS characteristic similar to the solid PEC sphere at lower frequencies, and the characteristic gradually shifts to that of the solid dielectric sphere at higher frequencies. This is due to the coating thickness being electrically significant at higher frequencies.

Next, monostatic RCS is computed for single-coated spherical surfaces to examine the effect of coating thicknesses at a constant frequency of 2.45GHz. As can be ob-



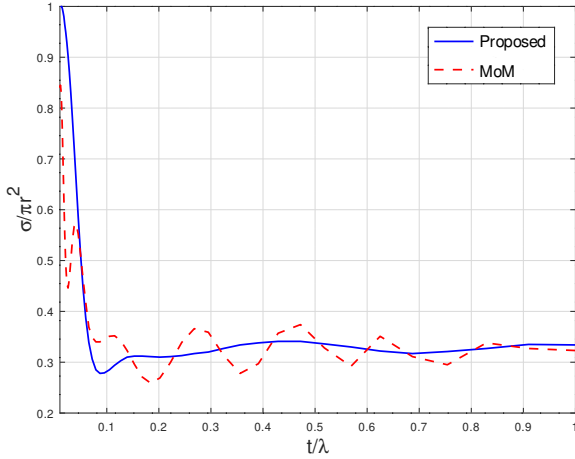


FIGURE 11: Normalized monostatic RCS w.r.t normalized coating thickness for a coated PEC sphere of diameter  $2\lambda$  with dielectric coating of  $\epsilon_r = 1.8$ ,  $\mu_r = 1.5$ ,  $\sigma = 10.2\omega\epsilon_0$  and  $\tan\delta = 5.6$ .

served in Fig. 11, when the coating thickness is greater than  $0.2\lambda$ , both proposed and MoM yielded a constant or nearly constant RCS value congruent to the flat coated surface.

Table. 1 and Table. 2 summarizes the computational efficiency of the proposed method for the structures studied. A tabulation of the comparative study of the computational time for the proposed method and MoM is given in Table. 1. The computational time is reduced by at least fifteen times for the proposed method compared to MoM, with good agreement between the computed values. In addition, for a double-coated structure, the computational time of MoM is approximately thirty times higher than the proposed method, see Table. 1. This is because the proposed method combines the field variation in the interfaces of each layer to create an equivalent value in contrast to discrete layer analysis in MoM.

Table. 2 gives a comparative study of the memory used by

TABLE 1: Comparative Study of Computational Time for Proposed Method vs. MoM

Structure	Coating	Proposed	MoM
Square plate	Single	144 s	2000 s
Square plate	Double	144 s	3282 s
Sphere	Single	123 s	1925 s

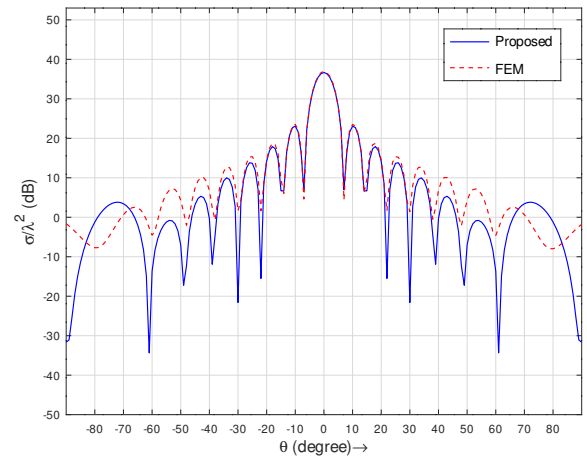
s = second

TABLE 2: Comparative Study of Memory Usage for Proposed Method vs. MoM

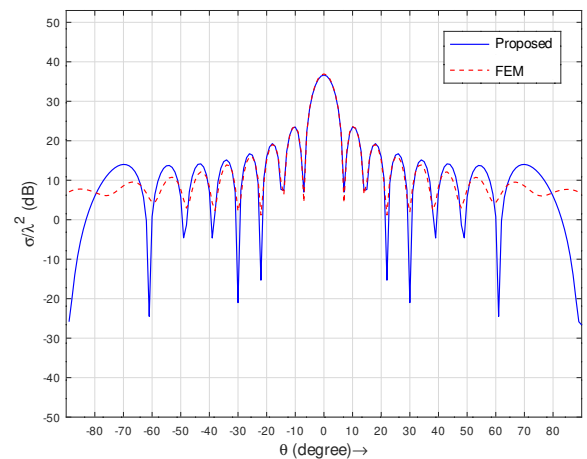
Structure	Coating	Number of surface		Mesh Size (GB)	
		Proposed	MoM	Proposed	MoM
Square plate	Single	1	11	11.46	195.29
Square plate	Double	1	16	11.46	450.19
Sphere	Single	1	2	12.9	25.8

the proposed method and MoM. As can be seen in Table. 2, the proposed method uses minimum number of surfaces in the form of 2D surface mesh in contrast to the 3D mesh used in full wave analysis. The proposed method not only reduces memory usage but also will not be influenced by the number of layers. The mesh size for the square plate with single as well as double layers is the same for the proposed method, whereas it is more than double for MoM, see Table. 2. Even though the proposed method can work efficiently with larger mesh facets, the facet size is kept constant for the fairness of the study.

The proposed method has also been validated using the finite element method (FEM), a well-developed method for the analysis of homogeneous multilayered media [22]. The bistatic RCS of a square plate with a side of  $8\lambda$  and a



(a)



(b)

FIGURE 12: Normalized bistatic RCS of coated PEC square plate of side  $8\lambda$  with modified epoxy coating ( $\epsilon_r = 3.7 - j0.05$ ,  $\mu_r = 1.39 - j3.56$  and dielectric loss tangent = 0.014) w.r.t observation angle  $\theta$  for normal plane wave incidence of a) TE polarization b) TM polarization.

single layer coating of ferrite-polymer thick film ( $\epsilon_r = 3.7 - j0.05$ ,  $\mu_r = 1.39 - j3.56$  and dielectric loss tangent = 0.014) of thickness  $0.2\lambda$  has been computed, see Fig. 12. The result for both TE and TM polarizations shows that the results from the proposed method agree with that of FEM analysis. It is to be noted that analysis using FEM for electrically large structures is time-consuming and need not always yield converging results [11]. While the FEM-based simulator [24] took an average of 25 minutes to compute the RCS for one polarization, the proposed method accomplished the same in approximately 4 minutes for both polarizations together.

#### IV. CONCLUSION

In this paper, a computationally efficient method for electromagnetic scattering analysis of electrically large multilayered lossy dielectric structures is presented and validated. The validation study in terms of radar cross-section computation showed the proposed method in good agreement with the method of moments (MoM) and the Finite element method (FEM). The proposed method uses significantly less memory and computation time in comparison to both MoM and FEM. The comparison study with MoM showed a reduction in computation time by a factor of fifteen and a minimum of fifty percent reduction in memory usage. The proposed method can be easily extended to study transmission and absorption in multilayer media with minimal modifications and inclusion of transmission coefficient in the modeling of the equivalent single-layer structure. Thus, facilitating analysis of non-metallic substrates, i.e., when the last layer of the multilayered structure is not PEC. Being computationally efficient the major advantage of the proposed method is the possibility of real-time analysis which is crucial in RCS applications like navigation, target characterization, etc. Also, the usage of 2D surface mesh and equivalent single-layer model reduces the memory requirement making the method suitable for onboard application with minimal hardware. Though the proposed method is validated using RCS the method is not limited to RCS computations. The method can be used for real-time scattering analysis in varied areas like material quality testing, bio-electromagnetic interactions, etc. that involve electrically large structures.

#### REFERENCES

- [1] Parul Mathur, Mauricio D. Perez, Robin Augustine, Dhanesh G. Kurup, "NDECOAX: A software package for nondestructive evaluation of stratified dielectric media," *SoftwareX*, vol. 9, pp. 187-192, 2019.
- [2] K. S. Keerthi., K. Ilango, and G. N. Manjula., "Study of Midfield Wireless Power Transfer for Implantable Medical Devices," in 2018 2nd International Conference on Biomedical Engineering (IBIOMED), pp. 44-47, 2018.
- [3] L. M., S. A., Menon SK, "A novel and effective technique to reduce electromagnetic radiation absorption on biotic components at 2.45 GHz," *Electromagn Biol Med*, vol. 44, no. 2, pp. 184-200, Apr 2022.
- [4] L. Meenu, S. Aiswarya and S. K. Menon, "A Survey on Heating Effects of Electromagnetic Radiation on Human Body," in 2020 5th International Conference on Computing, Communication and Security (ICCCS), mpp. 1-4, 2020.
- [5] Fan, Xiaoyan and Qin, Yufeng and Shang, She and Song, Dawei and Sun, Wenfeng and Li, Dong and Luo, Xi, "Research on the bistatic RCS characteristics of stealth aircraft," in 2015 Asia-Pacific Microwave Conference (APMC), vol. 3, pp. 1-3, 2015.
- [6] Y. Liu, Y. -T. Zheng, H. -J. Zhou, X. -J. Chen and X. -y. Guo, "A Hybrid Method Of FEBI And PO For Scattering Analysis Of Inhomogeneous Structures With Large-Scale Platform," in 2019 IEEE International Conference on Computational Electromagnetics (ICCEM), pp. 1-3, 2019.
- [7] Kaburcuk, F. "Fast Wideband Solutions Obtained Using Model Based Parameter Estimation With Method of Moments," in *Advanced Electromagnetics*, vol. 6, no. 3, pp. 13-17, Oct. 2017.
- [8] R. Khairi, A. Coatanhay, and A. Khenchaf, "Optimal High-Order Method of Moment combined with NURBS for the scattering by a 2D cylinder," in *Advanced Electromagnetics*, vol. 2, no. 1, pp. 33-43, Feb. 2013.
- [9] Y. Ren, M. Zhu, Q. Ren, Y. P. Chen and Y. Liu, "Efficient Electromagnetic Modeling of Multidomain Planar Layered Medium by Surface Integral Equation," in *IEEE Transactions on Microwave Theory and Techniques*, vol. 69, no. 8, pp. 3635-3644, Aug. 2021.
- [10] D. G. Kurup, "Analytical Expressions for Spatial-Domain Green's Functions in Layered Media," *IEEE Transactions on Antennas and Propagation* vol. 63, no. 11, pp. 4944-4951, 2015.
- [11] E. Y. Chow, Y. Ouyang, B. Beier, W. J. Chappell and P. P. Irazoqui, "Evaluation of Cardiovascular Stents as Antennas for Implantable Wireless Applications," in *IEEE Transactions on Microwave Theory and Techniques*, vol. 57, no. 10, pp. 2523-2532, Oct. 2009.
- [12] R. Kouyoumjian, L. Peters and D. Thomas, "A modified geometrical optics method for scattering by dielectric bodies," in *IEEE Transactions on Antennas and Propagation*, vol. 11, no. 6, pp. 690-703, Nov. 1963.
- [13] H. Kim and H. Ling, "Electromagnetic scattering from an inhomogeneous object by ray tracing," in *IEEE Transactions on Antennas and Propagation*, vol. 40, no. 5, pp. 517-525, May 1992.
- [14] D. Didascalou, T. M. Schafer, F. Weinmann and W. Wiesbeck, "Ray-density normalization for ray-optical wave propagation modeling in arbitrarily shaped tunnels," in *IEEE Transactions on Antennas and Propagation*, vol. 48, no. 9, pp. 1316-1325, Sep. 2000.
- [15] J. A. M. Lorenzo, A. G. Pino, I. Vega, M. Arias and O. Rubinos, "ICARA: induced-current analysis of reflector antennas," in *IEEE Antennas and Propagation Magazine*, vol. 47, no. 2, pp. 92-100, Apr. 2005.
- [16] C. A. Balanis, "Advanced Engineering Electromagnetics," 1<sup>st</sup> ed., New York: Wiley, 1989.
- [17] J. G. Meana, J. Á. Martínez-Lorenzo, F. Las-Heras and C. Rappaport, "Wave Scattering by Dielectric and Lossy Materials Using the Modified Equivalent Current Approximation (MECA)," in *IEEE Transactions on Antennas and Propagation*, vol. 58, no. 11, pp. 3757-3761, Nov. 2010.
- [18] [http://www.emagtech.com/wiki/index.php/V%26V\\_Article\\_2:\\_Computing\\_Radar\\_Cross\\_Section\\_Of\\_Metallic\\_Targets\\_Using\\_EM\\_Cube](http://www.emagtech.com/wiki/index.php/V%26V_Article_2:_Computing_Radar_Cross_Section_Of_Metallic_Targets_Using_EM_Cube)
- [19] K J Pascoe, "Reflectivity and Transmissivity through Layered, Lossy Media: A User-Friendly Approach", School of Engineering, Air Force Institute of Technology, Wright-Patterson Air Force Base, Ohio, 2001 [Online]. Available: <https://apps.dtic.mil/sti/pdfs/ADA389099.pdf>
- [20] Macleod, H.A., "Thin-Film Optical Filters," 3<sup>rd</sup> ed., Bristol and Philadelphia : IoP Pub., 1986.
- [21] J. Van-Bladel, *Electromagnetic Fields*, 2<sup>nd</sup> ed. NJ: IEEE Press/Wiley Interscience, 2007.
- [22] Y. Ren, Q. H. Liu and Y. P. Chen, "A Hybrid FEM/MoM Method for 3-D Electromagnetic Scattering in Layered Medium," in *IEEE Transactions on Antennas and Propagation*, vol. 64, no. 8, pp. 3487-3495, Aug. 2016.
- [23] Verma, A., Saxena, A. K., and Dube, D. C., "Microwave permittivity and permeability of ferrite-polymer thick films", *Journal of Magnetism and Magnetic Materials*, vol. 263, no. 1-2, pp. 228-234, 2003.
- [24] ANSYS@HFSS (High Frequency Simulation Software) version 15.0.0 <http://www.ansoft.com/products/hf/hfss/>